ELSEVIER
Chemical Engineering Journal 86 (2002) 193–198
Chemical Engineering Journal
www.elsevier.com/locate/cej

Drying behavior of polymer solution containing two volatile solvents

M. Yoshida*, H. Miyashita

Department of Materials Science and Engineering, Toyama University, 939-8555 Toyama, Japan

Abstract

A study on the drying of thin layers of polymer solution containing two volatile solvents is performed through experiments and numerical simulation. In the experiments, the individual drying rate of each solvent as well as the overall drying rate is obtained. The initial composition and the thickness of a sample are varied in order to examine their effects on the drying characteristics. Moreover, simulation is performed by solving a pair of diffusion equations for each solvent together with a heat balance equation. The diffusivity and the vapor pressure of solvents necessary for the simulation are estimated using free-volume theory of Vrentas and Duda and the Flory–Huggins equation, respectively. The results of simulation show qualitative agreement with experiments, while apparent mass transfer rate in the film is smaller than that estimated from diffusivity data found in the literature. The reason of underestimation is a future subject. © 2002 Published by Elsevier Science B.V.

Keywords: Multi-component; Polymer solution; Modeling; Heat and mass transfer

1. Introduction

Drying a coated layer of polymer solution plays an important role in industrial situations such as making functional films, special-effect printings and paint coatings. For the purpose of systematic design of dryers and elaborate control of products quality, many works have been performed on transport phenomena occurring during drying of coated films [1,2]. In these works, however, most of the researchers have restricted themselves to systems comprising two components—a polymer as a solute and a volatile solution. Although industrial drying frequently encounters polymer solutions containing multicomponent volatile solvents, only few studies have so far been made at such systems because of complexity in transport phenomena, for instance, cross-diffusion, non-Fickian behavior of diffusion, and interaction between contraction stress and diffusion rate. It is only in the last few decades that the study of these subjects has become active; some theories have been proposed [3–6] but few others are still in progress. Further investigation is necessary for practical applications in industry.

For the development of drying theories of multicomponent solution, it is very important to accumulate experimental data and to clarify to what extent one can predict the drying behavior without considering complicated phenomena described above. From this point of view, the authors have performed experiments on convective drying of ternary mixtures consisting of two volatile solvents and a polymer as a solute. In a previous paper, experimental results of polystyrene–toluene (TOL)–ethylbenzene (EB) and polystyrene–toluene–xylene systems are reported [7].

In this study, experiments are performed on convective drying of a thin layer of polyvinylacetate (PVAc)–TOL–EB system. The effects of the initial composition of a layer on the drying rate of each solvent and on the drying selectivity are investigated. The effect of the sample thickness is also discussed. Moreover, numerical simulation is performed using a simple model of heat and mass transfer to clarify its limitations.

2. Experimental

2.1. Experimental apparatus and procedure

In spite of the fact that polymer films manufactured by drying of polymer solution in industry usually have a thickness of several tens of microns, we performed experiments using layers of solution with an initial thickness of the order of millimeter. This is because tracing the change in weight is a very difficult procedure for a coated thin layer. The short duration time of drying is another reason. Since the mechanism of heat and mass transfer in a polymer solution is independent of the thickness unless compared with the molecular size, using thick samples is reasonable for the analysis of drying mechanism. In the experiments, drying

---

* Corresponding author. Tel.: +81-76-445-6836; fax: +81-76-445-6837.
E-mail address: myoshida@eng.toyama-u.ac.jp (M. Yoshida).

1385-8947/02/$ – see front matter © 2002 Published by Elsevier Science B.V.
PII: S1385-8947(01)00289-3

Nomenclature

C_p	heat capacity ($\mathrm{J\,kg^{-1}\,K^{-1}}$)
d	density of pure component ($\mathrm{kg\,m^{-3}}$)
D	diffusion coefficient ($\mathrm{m^2\,s^{-1}}$)
$\Delta_{\mathrm{vap}}H$	vaporization heat ($\mathrm{J\,kg^{-1}}$)
$j^{\bullet}$	mass flux relative to volume-average velocity ($\mathrm{kg\,m^{-2}\,s^{-1}}$)
k_{g}	mass transfer coefficient ($\mathrm{kg\,m^{-2}\,Pa^{-1}\,s^{-1}}$)
L	layer thickness (m)
P	vapor pressure (Pa)
t	time (s)
u	dry-based solvent content
U	overall heat transfer coefficient ($\mathrm{J\,m^{-2}\,Pa^{-1}\,s^{-1}}$)
$\hat{V}$	partial specific volume ($\mathrm{m^3\,kg^{-1}}$)
x	distance from bottom (m)

Greek symbols

ρ	mass concentration ($\mathrm{kg\,m^{-3}}$)
χ	polymer–solvent interaction parameter
ψ	solvent-based mass fraction
ω	mass fraction

Subscripts

a	air
A	lower-boiling solvent
B	higher-boiling solvent
eq	equilibrium value
i	interface
m	material
P	polymer
0	initial value

Superscripts

$*$	pure state
over line	mean value

conditions were selected carefully so as not to cause natural convection in a layer.

A schematic diagram of the experimental apparatus is shown in Fig. 1. A solution poured in a 5 cm × 5 cm tray is placed in a square hole of 5.5 cm × 5.5 cm bored in the bottom panel of the duct. The vertical position of the tray is adjusted so that the surface of the solution is initially at the same level with the bottom face of the duct. The tray is buried in a block of styrene foam for thermal insulation, and is placed on an electronic balance for real-time measurement of weight. The solution is dried with a horizontal flow of air heated to a desired temperature by two heaters.

During drying, the sample is weighted at certain time intervals in order to obtain an overall drying rate curve. Simultaneously, the temperatures of the sample are measured using thermocouples at the surface and bottom of the sample. The temperature of air adjacent to the sample is measured as well.

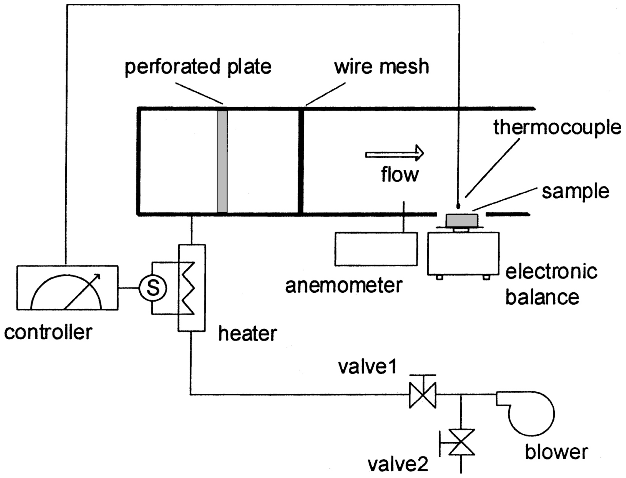

Fig. 1. Experimental apparatus.

Moreover, in order to obtain individual drying rates of each solvent, the change in mean composition of a sample is traced during drying. The measurement is performed by the following procedure: a sample is removed from the apparatus after a prescribed time since drying started, then dissolved in a dilutent, and finally analyzed using gas chromatography. Since a sample is all exhausted on analysis, resumption of drying with the same sample is impossible. It is hence necessary to repeat experiments again and again under the same condition with different drying times.

2.2. Experimental conditions

In this study, a system consisting of PVAc as a solute, TOL as a lower-boiling solvent, and EB as a higher-boiling solvent—will hereafter be indicated by P, A and B, respectively—is employed as a model solution. The initial composition of a solution is varied in a manner as shown in Table 1. The initial mass fraction of polyvinylacetate,

Table 1
Experimental conditions

No.	ω_{P0}	ω_{A0}	u_0	ψ_0	L (m)
1	0.17	0.00	5.0	0.0	0.003
2		0.17		0.2	
3		0.33		0.4	
4		0.50		0.6	
5		0.67		0.8	
6		0.83		1.0	
7	0.17	0.00	5.0	0.0	0.001
8		0.17		0.2	
9		0.33		0.4	
10		0.50		0.6	
11		0.67		0.8	
12		0.83		1.0	

denoted as ω_{P0}, is fixed at 0.17, while that of TOL, ω_{A0}, is varied from 0 to 0.83.

Since the mass fraction is not suitable for recognizing the residual amount of solvents intuitively, a dry-based solvent content, u, is defined as

$$u = \frac{\rho_A + \rho_B}{\rho_P} = \frac{\omega_A + \omega_B}{\omega_P} \tag{1}$$

where ρ_A, ρ_B and ρ_P are the mass concentration of component A, B and P in solution, respectively. The variable u means the ratio of the whole mass of solvents to the mass of polymer. Moreover, in order to discuss the composition of residual solvent in a layer, a solvent-based mass fraction of solvent I, ψ_I (I = A or B), is defined as

$$\psi_I = \frac{\rho_I}{\rho_A + \rho_B} = \frac{\omega_I}{\omega_A + \omega_B} \tag{2}$$

Then, a dry-based content of solvent I, u_I, is represented as

$$u_I = \psi_I u \tag{3}$$

In the experiments, fixing the initial value of dry-based solvent content, u_0, at 5.0, we varied the initial value of the solvent-based mass fraction of TOL, ψ_{A0}, from 0 to 1.

The air velocity is 2.5 m/s and the air temperature is 60 °C for all experiments. The humidity of the drying air, which is not controlled in this apparatus, is in the range of 0.01 ± 0.001 kg H_2O/kg dry air throughout the drying for all experiments.

3. Modeling

3.1. Physical model

Here we consider the drying of a layer of polymer solution placed on a flat plate. The solution consists of a polymer P, a lower-boiling solvent A, and a higher-boiling solvent B. Initially, the layer has a thickness of L_0 and a uniform temperature of T_0. The initial mass concentrations of P, A and B are ρ_{P0}, ρ_{A0} and ρ_{B0}, respectively. At time $t = 0$, the layer is suddenly exposed to a gas flow and solvents start to evaporate at the surface. The bottom of the layer is non-permeable and insulated thermally.

3.2. Mathematical model

In order to formulate heat and mass transfer equations, the following assumptions are introduced: (1) mass transfer is one-dimensional in the direction of the thickness; (2) the layer shrinks only in the direction of the thickness; (3) the temperature of the layer varies uniformly, i.e., heat transfer in the layer is ignored; (4) the shrinkage of the layer balances the loss in solvents, i.e., there is no volume change on mixing; (5) the volume average velocity is zero; (6) diffusion of solvents follows Fick's law and the cross-diffusion is negligible; (7) effects of contraction stress is ignored.

With these assumptions, the mass transfer during drying of a layer of polymer solution is described by the following set of equation [8]

$$\frac{\partial \rho_I}{\partial t} = \frac{\partial}{\partial x}\left(D_I \frac{\partial \rho_I}{\partial x}\right) \quad (I = A, B) \tag{4}$$

$$\frac{dL}{dt} = \left\{ \frac{\hat{V}_A D_A (\partial \rho_A/\partial x) + \hat{V}_B D_B (\partial \rho_B/\partial x)}{1 - \rho_A \hat{V}_A - \rho_B \hat{V}_B} \right\}\Bigg|_{x=L} \tag{5}$$

with the following initial conditions

$$\rho_I = \rho_{I0} \text{ at } t = 0 \text{ for } 0 < x < L_0 \tag{6}$$

$$L = L_0 \text{ at } t = 0 \tag{7}$$

Boundary conditions at the bottom are described as

$$\frac{\partial \rho_I}{\partial x} = 0 \quad \text{at } x = 0 \tag{8}$$

On the other hand, for boundary conditions at the surface, two types of equations are properly applied depending on values of mass concentration of solvents at the surface. Until the surface concentration reaches its equilibrium value, the resistance of the gas film dominates the mass transfer rate, and boundary conditions at the surface are given by the following equations:

$$j^{\bullet}{}_{I,s} = k_{gI}(p_{I,i} - p_{I,a}) \tag{9}$$

where $j^{\bullet}{}_I$ is the mass flux of component I relative to the volume-average velocity, and its value at surface $j^{\bullet}{}_{I,s}$ equals to individual drying rate of component I:

$$j^{\bullet}{}_{I,s} = -\frac{d(\bar{\rho}_I L)}{dt} \tag{10}$$

Once the surface concentration reaches its equilibrium value, it henceforth remains unchanged:

$$\rho_I = \rho_{I_{eq}} \quad \text{at } x = L \tag{11}$$

moreover, heat balance is represented by the following ordinary differential equation:

$$U(T_a - T_m) = L(\bar{\rho}_A C_{pA} + \bar{\rho}_B C_{pB} + \bar{\rho}_P C_{pP}) \frac{dT_m}{dt} + (\Delta_{vap} H_A j^{\bullet}{}_A + \Delta_{vap} H_B j^{\bullet}{}_B) \tag{12}$$

with the following initial condition:

$$T_m = T_{m0} \quad \text{at } t = 0 \tag{13}$$

The set of Eqs. (4)–(13) is solved numerically by combining the Crank–Nicolson finite difference method with the Runge–Kutta–Gill method.

3.3. Evaluation of diffusivity and vapor pressure

If it is assumed that the concentration dependence of the partial specific volumes of all components is negligible, the self-diffusion coefficients of the two solvents can be expressed as [8]

Table 2
Free volume parameters of each component

Component	D_{0I} (m^2/s)	$\hat{V}_I^*$ (cm^3/g)	ξ_{IP} (−)	K_{1I}/γ (cm^3/g K)	K_{2I}–T_{gI} (K)	χ_{IP} (–)
A (TOL)	4.82×10^{-8}	0.917	0.82	1.45×10^{-3}	−86.32	0.393
B (EB)	4.61×10^{-8}	0.946	1.028	1.40×10^{-3}	−80.01	0.385
S (PVAc)	–	0.728	–	4.33×10^{-4}	−258.2	–

$$D_A = D_{0A}\exp\left\{-\frac{\omega_A\hat{V}_A^* + \omega_B\hat{V}_B^*(\xi_{AP}/\xi_{BP}) + \omega_P\hat{V}_P^*\xi_{AP}}{\hat{V}_{FH}/\gamma}\right\} \tag{14}$$

$$D_B = D_{0B}\exp\left\{-\frac{\omega_A\hat{V}_A^*(\xi_{BP}/\xi_{AP}) + \omega_B\hat{V}_B^* + \omega_P\hat{V}_P^*\xi_{BP}}{\hat{V}_{FH}/\gamma}\right\} \tag{15}$$

where D_{0A} and D_{0B} are constants, and $\hat{V}_{FH}/\gamma$ is defined as

$$\begin{aligned}\frac{\hat{V}_{FH}}{\gamma} &= \frac{K_{1A}}{\gamma}(K_{2A}+T-T_{gA})\omega_A \\ &\quad + \frac{K_{1B}}{\gamma}(K_{2B}+T-T_{gB})\omega_B \\ &\quad + \frac{K_{1P}}{\gamma}(K_{2P}+T-T_{gP})\omega_P\end{aligned} \tag{16}$$

In the above equation, T_{gI} is the glass transition temperature of component I, and parameters of $\hat{V}_I^*$, ξ_{IP}, γ, K_{1I} and K_{2I} is concerned with the free volume theory [8]. Here we only show the values of these parameters used for calculations in Table 2 (refer to [9,10] for details).

The vapor pressure at surface for given solvent content and temperature is estimated using the following equation obtained by modifying the Flory–Huggins equation:

$$P_I = P_I^*\psi_I(1-\gamma_P)\exp(\gamma_P + \chi_{IP}\gamma_P^2) \tag{17}$$

where γ_P is the volume fraction of the polymer, and χ_{IP} is the polymer–solvent interaction parameter. The value of χ_{IP} for each solvent is given in Table 2.

4. Results and discussion

4.1. One polymer–one solvent system

First of all, drying of a polymer solution containing a single solvent is discussed using Fig. 2, where experimental drying rate and temperature curves when $L_0 = 3$ and 1 mm are plotted for PVAc–TOL and PVAc–EB systems. Simulated results are also plotted for comparisons.

The drying rates for two different initial thickness show almost the same value in the beginning of drying, which suggests that the mass transfer rate is dominated by the resistance of the gas film. After a period during which the drying rate is almost constant, the drying rate starts decreasing rapidly. Then, exhibiting linear decrease with $\bar{u}$ for a while, the drying rate abruptly changes its decreasing rate, and the drying rate curve shows a bending. This feature is more prominent for thicker layers.

Solid and broken lines in the figure show simulated drying rate and temperature curves. Results of simulation give larger drying rates than experimental ones as a whole, although the layer temperature is estimated to be lower. Since the lower temperature leads to lower values of diffusivity and hence smaller drying rates, the overestimation

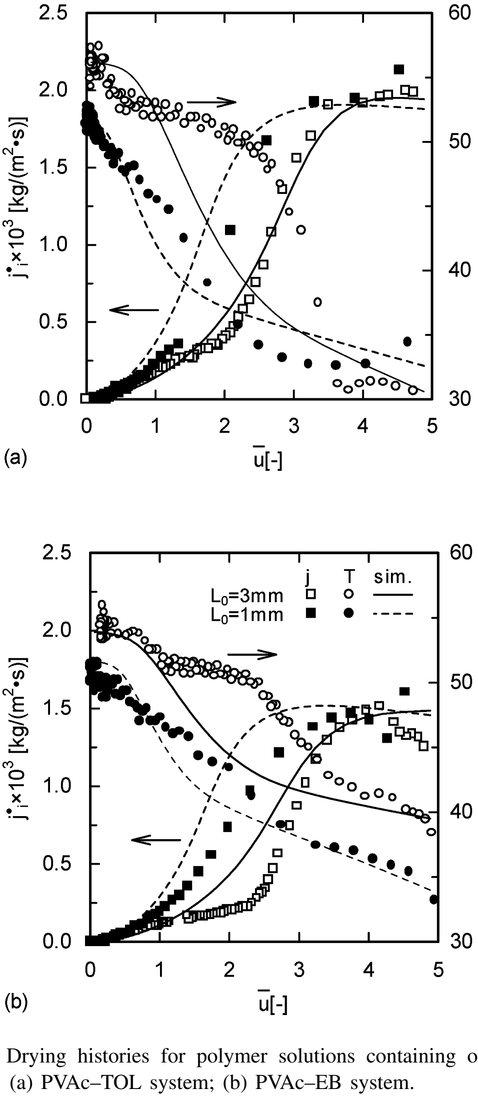

Fig. 2. Drying histories for polymer solutions containing one volatile solvent: (a) PVAc–TOL system; (b) PVAc–EB system.

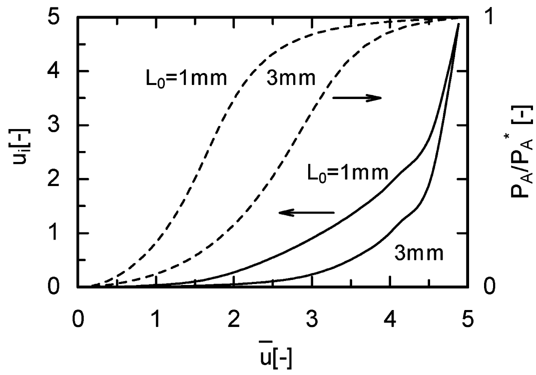

Fig. 3. Change in concentration at surface for PVAc–TOL solution (simulated).

of drying rate cannot be attributed to the underestimation of the layer temperature. Considering that the diffusivity of TOL and EB calculated by Eqs. (14) and (15) agrees well with experimental values [11], it seems to be probable that the effective diffusion rate is lowered by something such as the contraction stress due to shrinkage, and heterogeneity due to formation of microstructure.

In order to interpret characteristics of the drying rate curve from a viewpoint of mass transfer resistance, the relation between the solvent content at surface and the mean solvent content is plotted in Fig. 3 using numerical results for PVAc–TOL solution. When $L_0 = 3\,\mathrm{mm}$, though the solvent content at surface, u_i, decreases rapidly and falls to 20% of its initial value at about $\bar{u} = 4$, the corresponding relative pressure decrease only by 5% this time. Thus, the drying rate, related to vapor pressure by Eq. (9), is kept almost constant in the beginning. As drying proceeds, the relative pressure decreases gradually and hence the drying rate does. Moreover, u_i reaches approximately zero at about $\bar{u} = 2$, which corresponds to the bending of drying rate curve. Thus one can conclude that the drying rate after the bending is controlled by internal mass transfer resistance. When the initial thickness is small, the external resistance is relatively large, resulting in a mild drying with slower decrease in the solvent content at surface. Thus, the decrease in drying rate is more moderate, and it takes longer time before the internal mass transfer resistance takes the place of the external one.

4.2. One polymer–two solvent system

Fig. 4(a) shows experimental drying rate curves for solutions of PVAc–TOL–EB differing in initial composition. Curves have a similar shape to that for polymer–solvent systems. It was confirmed that the relation between the drying rate and the surface solvent content is also similar to that for polymer–solvent systems. The higher the initial vapor pressure of the solution, the higher is the initial value of the overall drying rate. However, no correlation was found between them in the period when the internal resistance was dominant. This implies that an optimum composition exists to minimize the drying time. Simulated results shown in Fig. 4(b) show tendency similar to experimental data, still insufficient in accuracy. The overestimation of drying rate is observed again during the period when the internal resistance is dominant.

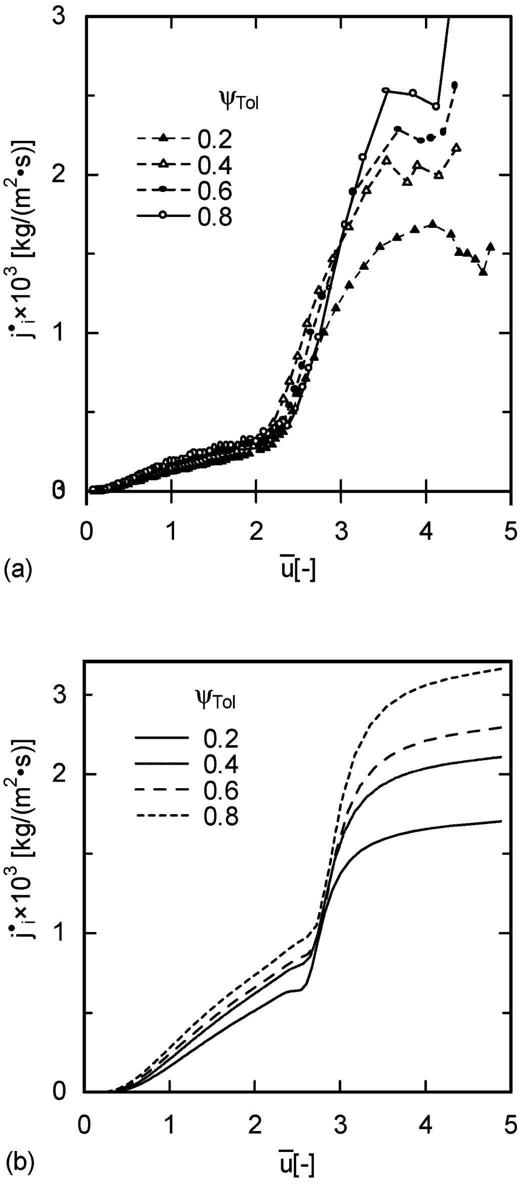

Fig. 4. Effect of initial composition on drying rate for PVAc–TOL–EB solution of $L_\mathrm{i} = 3\,\mathrm{mm}$: (a) experimental; (b) simulated.

Fig. 5 shows individual drying rate curves for $\psi_{\mathrm{A}0} = 0.6$. In this case, the drying rate of A is superior to that of B in the beginning and becomes almost the same as that of B. When $\psi_{\mathrm{A}0}$ is small, it happens that the drying rate of A greater than that of B in the beginning and is overtaken by that of B when the internal resistance becomes dominant. This is because the higher the initial drying rate, the faster is the decrease in the surface concentration and hence in the vapor pressure, resulting in a rapid decrease in the drying rate.

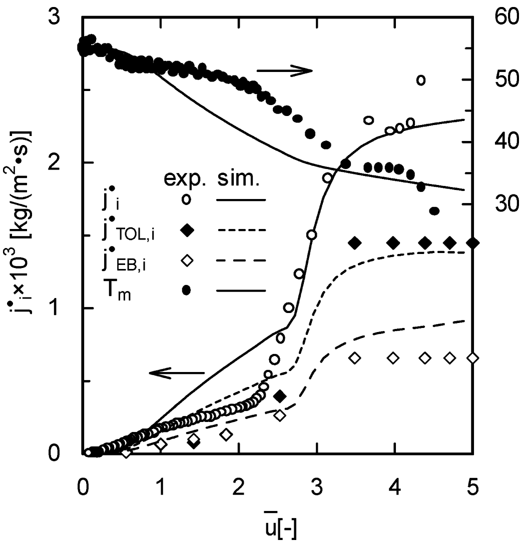

Fig. 5. Comparison of simulated drying history for TOL = 0.6 with experimental results.

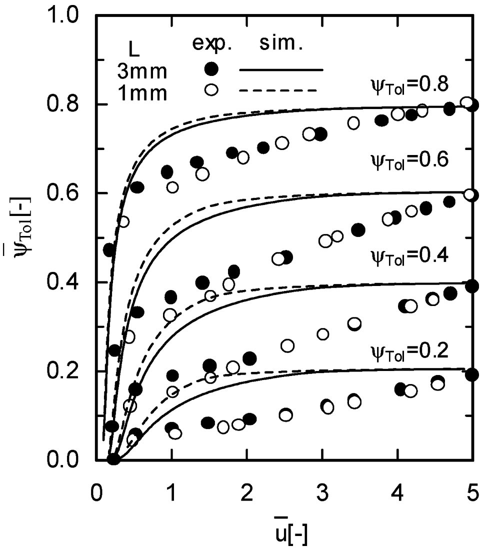

Fig. 6. Change in mean composition.

Fig. 6 shows changes in the solvent-based mass fraction of TOL with the mean solvent content. The slope of curves is positive throughout the drying irrespective of the initial composition and the thickness of the layer. In other words, TOL is removed preferentially and EB is enriched in the solution. When the internal resistance of mass transfer starts to dominate the drying rate, the effect of the initial thickness on the selectivity appears.

5. Conclusions

Drying of a thin layer of polymer solution containing two volatile solvents was studied experimentally and numerically. The process can be divided into three periods in view of mass transfer mechanism. At first, the drying rate is dominated by the external mass transfer resistance and is almost constant. Then the drying rate decreases rapidly, although it is still dominated by the external resistance. Finally, the internal resistance becomes dominant and the drying rate decreases gradually. The lower-boiling solvent is always removed preferentially and its selectivity is almost constant irrespective of the initial composition and the thickness of the layer. Numerical simulation can properly explain experimental results such as overall and individual drying rates and the selectivity, while the accuracy of estimation is not satisfactory because the diffusion rates of solvents are overestimated if diffusion in the literature is used. This suggests that the effective diffusivity is lowered by the contraction stress, the formation of microstructure or something. Elucidation of the cause and modeling is a future subject.

References

[1] M. Okazaki, K. Shioda, K. Masuda, R. Toei, Drying mechanism of coated film of polymer solution, J. Chem. Eng. Jpn. 7 (1974) 99.

[2] Y. Sano, S. Yamamoto, Mutual diffusion coefficient of aqueous sugar solution, J. Chem. Eng. Jpn. 26 (6) (1993) 633.

[3] R. Taylor, Film models for multicomponent mass transfer: computational methods. II. The linearised theory, Comp. Chem. Eng. 6 (1982) 69–75.

[4] D. Berthet, A. Bakhouya, J. Bouzon, J.M. Vergnaud, Drying of polymers, Modeling with diffusion–evaporation and shrinkage, Drying'92, 1992, pp. 364–373.

[5] F. Luna, J. Martínez, Stability of the ODE system describing continuous gas-phase controlled drying of a liquid film, Drying'98, 1988, p. 272

[6] D. Bruneau, M. Younis, An experimental and modeling approach of the drying of an initially fluid multiphase multicomponent medium, in: Proceedings of the 11th International Drying Symposium, 1998, p. 126.

[7] M. Yoshida, H. Miyashita, Convective drying of polymer solution containing two volatile solvents—effect of initial composition on drying rate and on selectivity, in: Proceedings of the 11th Annual Meeting of the Polymer Processing Society, 1995, p. 175.

[8] J.S. Vrentas, J.L. Duda, H.-C. Ling, Enhancement of impurity removal from polymer films, J. Appl. Polym. Sci. 30 (1985) 4499–4516.

[9] J.L. Duda, J.S. Vrentas, S.T. Ju, H.T. Liu, Prediction of diffusion coefficients for polymer–solvent systems, AIChE J. 28 (1982) 279.

[10] J.M. Zielinski, J.L. Duda, Predicting polymer/solvent diffusion coefficients using free volume theory, AIChE J. 38 (3) (1992) 405–415.

[11] Ju, S.T., Oscillatory and transient sorption studies of diffusion in polyvinyl acetate, Ph.D. Thesis, The Pennsylvania State University, University Park, PA, 1981.